

Corrosion of Cement Paste Coated Steel Bars in Marine Environment

Mohammed Tarek Uddin^{1,*}, Hidenori Hamada², Mohammed Abdullah Al Mamun³, and Ariful Hasnat⁴

¹*Professor, Department of Civil Engineering, University of Asia Pacific, Bangladesh*

²*Professor, Department of Civil Engineering, Kyushu University, Japan*

³*Doctoral Student, Department of Civil Engineering, Hokkaido University, Japan*

⁴*Research Associate, Department of Civil Engineering, University of Asia Pacific, Bangladesh*

**House No. 8/A, Road No. 7, Dhanmondi R/A, Dhaka-1205, tarek@uap-bd.edu, h-hamada@doc.kyushu-u.ac.jp, mamun.mohammed.maintenance@gmail.com, hasnat@uap-bd.edu*

ABSTRACT

A detailed experimental investigation was carried out to understand the performance of different cement paste coated steel bars against chloride-induced corrosion. Cylinder concrete specimens of diameter 100 mm and height 200 mm were made with steel bars embedded in concrete at a cover depth of 20 mm. Twenty-two separate cases were made with and without cement paste coated steel bars. W/C ratio of cement paste was varied from 0.3 to 1.0. After curing for one-month, the specimens were exposed to an accelerated chloride-induced corrosion environment. Each cycle of exposure consists 3.5 days under seawater exposure at 60°C and 3.5 days drying under atmospheric exposure. The specimens were tested after 10, 20, and 45 cycles of exposure. The test items include compressive strength of concrete, chloride ingress into concrete (acid soluble and water soluble chloride content), electrochemical evaluation of corrosion (half cell potential, polarization resistance of steel bars, concrete resistance, and anodic polarization curves), microscope investigations of steel-concrete interface, and physical evaluation of corrosion (corroded area, pit depth, weight loss) over the steel bars.

Based on this investigation, it is revealed that time to initiate corrosion is significantly increased for cement paste coated steel bars, particularly for coating with a low W/C. It is understood that chloride threshold limit for initiation of corrosion over the steel bars is significantly influenced by the nature of the steel-concrete interface around steel bars. The relationship between water soluble chloride content in concrete and acid soluble chloride content in concrete is also proposed.

Keywords: Corrosion, Coating, Cement Paste, Steel Bar, Marine Environment, Chloride Induced Corrosion.

INTRODUCTION

Deterioration of marine concrete structures caused by the corrosion of steel bars is a common problem. During construction, the steel bars were covered with mill scale, and in some cases also has brown rust due to rainwater or weathering for a short period in humid air, or black rust due to prolonged exposure to the atmosphere. For laboratory tests, polished

bars (cleaned by sand blasting or chemical method) are commonly used. Based on a study on different surface conditions of steel bars, Li and Sagues, 2001 concluded that removal of mill scale or rust from the steel surface by sandblasting is beneficial in elevating the chloride corrosion threshold in alkaline solution, although the corrosion rate of sandblasted steel after pitting initiation is higher than those of the mill-scaled and pre-rusted steel bars. Novak, et al., 2001 reported that pre-rusted steel bars in concrete, even without any chloride content, shows technically unacceptable average corrosion rate. Avial-Mendoza et al., 1994 also found a very high corrosion rate for the rusted steel bars. On the other hand, Al-Tayyib et al., 1990 reported that the initial rusting does not have an adverse effect on the corrosion resistance of reinforcing bar embedded in concrete, which contradicts with the results obtained by Li and Sagues, 2001; Novak et al., 2001; and Mendoza et al., 1994. No comparison of the steel-concrete interface was made in any of the previous studies to clarify the effect of physical nature of the steel-concrete interface, which is found to be an important factor regarding chloride-induced corrosion of steel bars in concrete (Mohammed et al, 1999, 2002a, 2002b). With this background, this study was planned.

EXPERIMENTAL METHOD

Materials

Normal Portland cement (NPC) was used. Physical properties and chemical analysis of cement are given in Table 1. Crushed granite and river sand were used. The properties of aggregate are given in Table 2. Japanese Industrial Standard (JIS) steel bars were used and its chemical properties are given in Table 3.

Table1. Physical and Chemical Composition of Cement

Specific Gravity	3.15
Blaine Fineness, cm ² /g	3190
Ignition Loss, %	0.7
SiO ₂ , %	21.3
Al ₂ O ₃ , %	5.3
CaO, %	64.4
MgO, %	2.2
SO ₃ , %	1.9

Table 2. Aggregate Properties

	Specific Gravity	Absorption (%)	Fineness Modulus
Sand	2.6	2.32	2.91
Gravel	2.65	0.65	6.31

Table 3. Chemical Compositions of Steel Bars

C (%)	Si (%)	Mn (%)	P (%)	S (%)
0.11	0.13	0.51	0.34	0.28

Specimen

Mixture proportions of concrete are summarized in Table 4. W/C was 0.5. Mixing water was potable tap water. Twenty-two cases were investigated. Concrete for each specimen was same and follows the mixture proportion summarizes in Table 4. The layout of the specimens

is shown in Figure 1. The length of the steel bars was 100 mm and 9 mm in diameter. Two round steel bars were placed at cover depth of 20 mm. Electric wires were connected with the steel bars and a cement paste coat of 0.25 mm thick was applied over the steel bars before embedding the steel bars inside concrete as shown in Figure 2. Variations of steel-concrete interface (denoted by C1~C22) were introduced by different types of cement, different W/C ratio, and different type of water. Ordinary portland cement, slag cement Type B (SCB, slag content varied from 30%~60%), slag cement Type C (SCC, slag content >60%), fly ash cement Type B (FACB, fly ash content 10%~20%), alumina cement, ordinary portland cement with silica fume, and ordinary portland cement with metakaoline were used for coating over steel bars. The properties of these materials are shown in Table 5. Tap water and seawater was used as mixing water. Tap water was used for all cases and seawater was used for alumina cement only. Preparation of cement paste is shown in Figure 3. After preparation of the cement paste, steel bars were submerged into the cement paste and carefully removed so that a layer of cement paste is formed over the steel bar. Then steel bars were hanged as shown in Figure 4 in a humid room. Then steel bars were hanged into the mold and then concrete was casted accordingly. The details of twenty-two cases are summarized in Table 6. Three types of concrete were used based on compaction procedure and slump value. These are noted as CON1, CON2, and CON3. In CON1, compaction was done by using a vibrator. In CON2, compaction was done by temping rod only. In CON3, a relatively low slump concrete was used and compaction was done by temping rod only. Cases related to the variation of steel-concrete interface denoted as C1 to C16 were made with CON1, and C17~C19 were made with CON2, and C20~C22 were made with CON3, respectively. After standard curing of 28 days, to accelerate the chloride ingress into concrete, the specimens were submerged in seawater of temperature 60°C for 3.5 days and then air-dried for 3.5 days under atmospheric temperature. During drying process, air circulation was provided by the electric fans. Natural seawater was used and its chemical and physical properties are given in Table 7.

Table 4. Mixture Proportion of Concrete

	G _{max} mm.	Slump Cm.	Air %	W/C	S/(S+G) %	W Kg/m ³	C Kg/m ³	S Kg/m ³	G Kg/m ³	AEWRA Kg/m ³	AEA g/m ³
NPC	15	8±1	4±1	0.5	43	174	348	741	1005	0.87	8.70

Note: AEA: Air-Entraining Admixture, AEWRA: Air-Entraining and Water Reducing Admixture

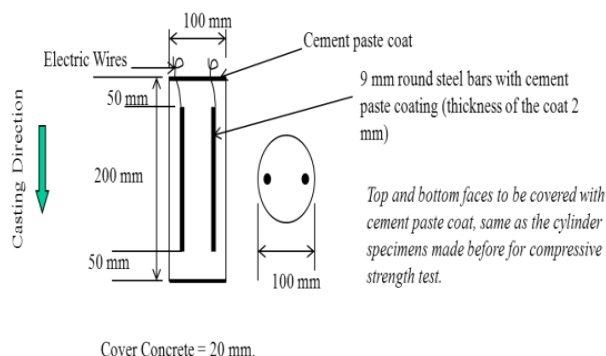


Figure 1. Layout of the specimen



Figure 2. Steel bars before embedded into the specimen

Table 5. Physical and Chemical Composition of Materials Used for Coating

	OPC	Blast furnace slag	Fly ash	Alumina Cement	Silica Fume	Metakaoline
Specific Gravity	3.15	2.88	2.24	3.08	2.26	2.46
Blaine Fineness (cm ² /g)	3370	4180	4020	4630	22.5 (m ² /g) BET	31960
Ignition Loss (%)	1.96	0.95	2.3	0.2	2.0	-
SiO ₂ (%)	-	-	-	3.0	93.0	-
Al ₂ O ₃ (%)	-	-	-	57.1	-	-
CaO	-	-	-	33.0	-	-
MgO (%)	1.42	5.71	-	0.3	0.7	-
SO ₃ (%)	1.86	1.98	-	-	0.3	-
Fe ₂ O ₃ (%)	-	-	-	1.1	-	-

-Not available



Figure 3. Mixing of cement paste



Figure 4. Drying of steel bars after application of cement paste coating

Table 6. Composition of the Total Specimens

Coating Material	Method of Compaction	Without Cement Paste	W/C of Cement Paste Coat				Type of Concrete
			0.3	0.5	0.7	1.0	
1. OPC	Compaction by Vibrator	C1	C2	C3	C4	C5	CON1
2. SCB	Compaction by Vibrator			C6			
3. SCC	Compaction by Vibrator			C7			
4. FACB	Compaction by Vibrator			C8			
5. Alumina Cement (seawater mixing)	Compaction by Vibrator		C9	C10			
6. Alumina Cement (tap water mixing)	Compaction by Vibrator		C11	C12			
7. OPC+Silica Fume (10%)	Compaction by Vibrator		C13	C14			
8. OPC+Metakaoline (5%)	Compaction by Vibrator		C15	C16			
9. OPC	Compaction by Rodding	C17	C18	C19			CON2
10. OPC (concrete slump 4-5 cm)	Compaction by Rodding	C20	C21	C22			CON3

Table 7. Physical Properties and Chemical Composition of Seawater

Specific Gravity	pH	Na ppm	K ppm	Ca Ppm	Mg ppm	Cl Ppm	SO ₄ ppm	CO ₃ ppm
1.022	7.77	9290	346	356	1167	17087	2378	110

METHOD OF EVALUATION

Compressive Strength

Cylindrical specimens were made to measure compressive strength of concrete at 28 days. The compressive strengths of the concrete specimens were determined as per Japanese Industrial Standard JIS-A1108.

Half-Cell Potential

Half-cell potential were measured by Ag/AgCl half-cell at the exposure age of 10, 20, and 45 cycles. Before measuring half-cell potential, the specimens were kept under water for 24 hours at a temperature of 20°C.

Micro-Cell Corrosion

Micro-cell corrosion current over the steel bars was measured at 10, 20, and 45 cycles of exposure by using AC impedance method. The low frequency was set at 10 mHz and high frequency at 20 Hz. The following equation was used to calculate the micro-cell current density (Fontana and Greene, 1983).

$$I_{mic} = \frac{B}{R_p} \times 10^6 \quad (1)$$

Where, I_{mic} is the micro-cell current density in $\mu\text{A}/\text{cm}^2$, $B= 0.026$ V and R_p is the polarization resistance in $\Omega.\text{cm}^2$.

Anodic Polarization Curves

Anodic polarization curves of the steel bars were measured at 10, 20, and 45 cycles of exposure. For this, the natural potential of the steel bars shifted to +1V gradually at the scanning speed of 1mV/Sec and the corresponding anodic current was measured. The specimens were submerged in seawater during the measurement. Ag/AgCl half-cell was used to measure the anodic polarization curves. The passivity grades of the steel bars was evaluated based on the anodic polarization curves (Otsuki et al., 1992). The method is explained below:

1. When the anodic current density is over $100 \mu\text{A}/\text{cm}^2$ at least at one point between +0.25 and + 0.65V (versus Ag/AgCl) of anodic polarization curve, then the passivity grade is defined as 0. The 0 passivity grade means complete loss of passivity, that is, no passivity;
2. When the anodic current density is 10 to $100 \mu\text{A}/\text{cm}^2$ between +0.25 and +0.65 V (versus Ag/AgCl) of the anodic polarization curve, then the passivity grade is defined as 1. This passivity grade means some degree of passivity, which is better than no passivity;
3. When the anodic current density is over $10 \mu\text{A}/\text{cm}^2$ at least at one point between +0.25 and +0.65 V (versus Ag/AgCl) of anodic polarization curve, then the passivity grade is defined as 2. This passivity grade means some degree of passivity, which is better than the passivity Grade 1;

4. When the anodic current density is 1 to 10 $\mu A/cm^2$ between +0.25 and +0.65 V (versus Ag/AgCl) of anodic polarization curve, then the passivity grade is defined as 3. This passivity grade means some degree of passivity, which is better than the passivity Grade 2;

5. When the anodic current density is over 1 $\mu A/cm^2$ at least at one point between +0.25 and +0.65 V (versus Ag/AgCl) of anodic polarization curve, then the passivity grade is defined as 4. This passivity means some degree of passivity, which is better than the passivity Grade 3; and

6. When the anodic current density is less than 1 $\mu A/cm^2$ between +0.25 and +0.65 V (versus Ag/AgCl) of anodic polarization curve, then the passivity grade is defined as 5. This passivity means excellent passivity.

The more is the number of passivity grades, the better the passivity is.

Chloride Concentration

Plain concrete specimens were used to measure chloride ingress into concrete at the exposure age of 10, 20, and 45 cycles. To measure chloride content, concrete samples were collected from 5 mm around the steel bar for each case. Also a 20 mm disc was cut to measure the chloride profile of C1, C17, and C20 from the middle portion of the specimen. It was cut again to take samples from the depths of 0~5, 8~18, 21~31, 34~44, and 47~53 mm. The samples were powdered by a vibrating mill. Water soluble and acid soluble chloride content was measured as per JCI-SC4.

Visual and Microscopic Investigation

After electrochemical investigation at 10, 20, and 45 cycles, the specimens were split opened. The condition of the steel bars and the surrounding concrete was checked visually. Corroded area over the steel bars was traced over a transparent paper and then the area was quantified by a digital planimeter. Optical microscope was used to visualize the condition of the steel-concrete interface. The interface was enlarged by 25 ~ 175 times.

The physical nature of steel-concrete interface was also investigated by Scanning Electron Microscope (SEM). Also, size and distribution of voids around steel-cement interface were evaluated by linear traversing. These data are not incorporated in this report due to limited space.

RESULTS AND DISCUSSION

Compressive Strength

The average compressive strengths of concrete were 45.85 MPa, 44.86 MPa, and 39.43 MPa for CON1, CON2, and CON3, respectively.

Water Soluble Chloride Concentration

Water soluble chloride concentration as % of cement mass at 10, 20, and 45 cycles of exposure are shown in Figure 5, Figure 6, and Figure 7 respectively for CON1, CON2, and CON3. Chloride threshold limit is generally defined at 0.4% of cement mass (RILEM, 1988). For all cases, chloride concentration into concrete is increased with time. Maximum chloride ingress into concrete is found for the case with low slump concrete and compaction

by rodding only. It is expected due to the presence of more capillary channels in concrete compacted by rodding only. The state of corrosion of steel bars inside concrete is explained below with respect to the chloride concentration around steel bars.

Water soluble chloride concentrations around the steel bar are shown in Figure 8. The samples were collected from a distance 5 mm around the steel bars. After 10 cycles of exposure, it is found that chloride concentration of each case is below the chloride threshold level except for C1 and C4. After 20 cycles of exposure, it is found that chloride concentration around steel bar crosses the chloride threshold limit for C1-C4, C6, C7, C10, C14, C15 - C17, and C21. Mineral admixtures were used to make coat over the steel bars for C6-C8, and C13-C16. A dense steel-concrete interface is formed around the steel bars for these cases, which prevent steel bars from corrosion even for high chloride content. This is explained later.

Acid Soluble Chloride Concentration

Acid soluble chloride concentration as % of cement mass at 45 cycles of exposure is shown in Figure 9 for CON1, CON2, and CON3. Same as water soluble chloride, more ingress of acid soluble chloride concentration is found for the cases with low slump concrete and compaction with rodding only.

Acid soluble chloride concentrations for all cases around the steel bar are shown in Figure 10. Acid soluble chloride concentration around steel bar exceeds 0.75% of cement mass irrespective of all cases. However, relatively less amount of chloride is found for the cases coated with a low W/C.

Variation of water-soluble chloride concentration and acid soluble chloride concentration is shown in Figure 11. The following relationship is found between water-soluble (WS) chloride concentration and acid-soluble (AS) chloride concentration.

$$Y = 0.708 \times X \quad (2)$$

where, Y is the water-soluble chloride concentration in % of cement mass and X is the acid soluble chloride concentration in % of cement mass.

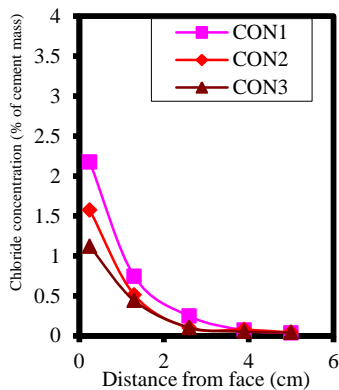


Figure 5. WS Cl⁻ concentration at 10 cycles

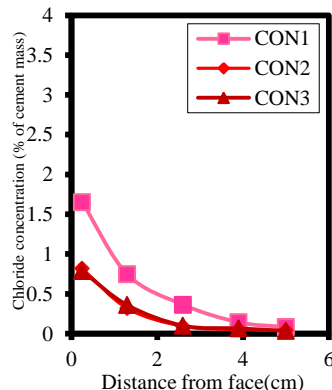


Figure 6. WS Cl⁻ concentration at 20 cycles

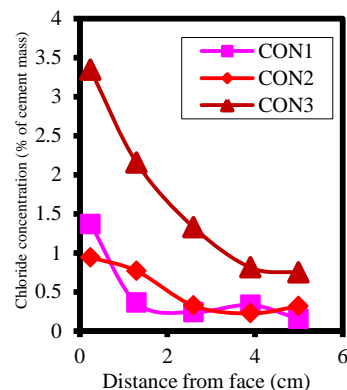


Figure 7. WS Cl⁻ concentration at 45 cycles

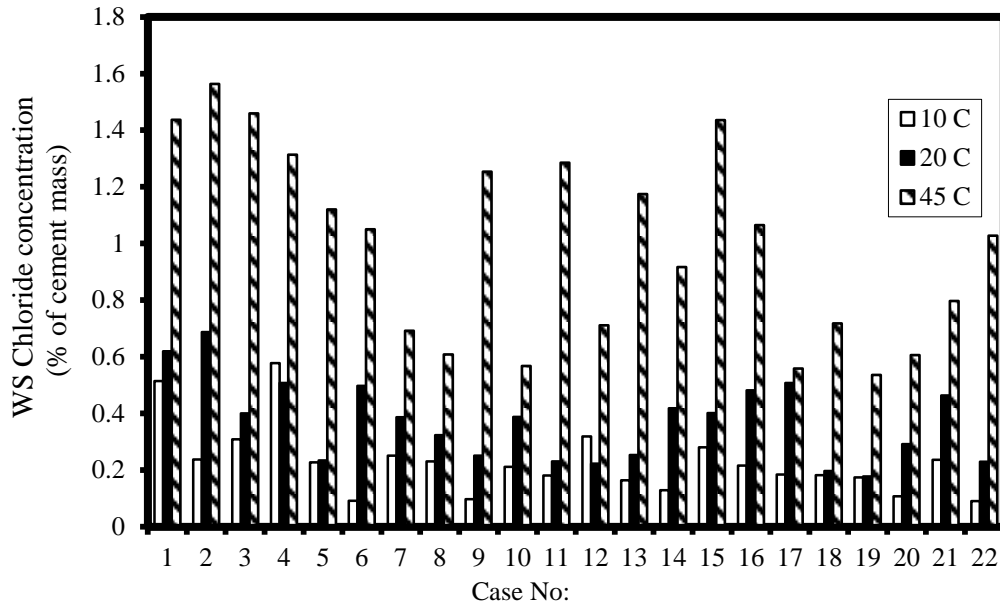


Figure 8. WS Cl⁻ concentration at 10C, 20C, 45C

Half-Cell Potential

Half-cell potential (HCP) over the steel bars is shown in Figure 12. The threshold limit of half-cell potential is assumed to be -230 mV (versus Ag/ AgCl) (ASTM C876, 1991). The half-cell potential before accelerated exposure was higher than -230 mV for all cases. After 10 cycles of exposure, C1, C6, C9, C10, C11, and C12 show the most negative half-cell potential compared to the others. For C1, no coating was applied. For C6, slag cement of Type B (SCB) was used to make coating over steel bar with W/C=0.5. For C9, C10, C11, and C12, alumina cement was used to make coat over steel bars. After 45 cycles of exposure all cases show lower negative potential than threshold limit of -230 mV except for C18, where the steel bars were coated with cement paste of ordinary portland cement (OPC) with a W/C ratio of 0.3 and C3 shows most negative potential, where the steel bars were coated with cement paste of ordinary Portland cement (OPC) with W/C ratio of 0.5.

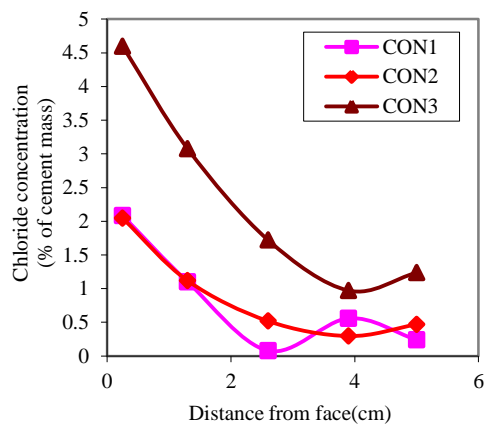


Figure 9. AS Cl⁻ concentration at 45 cycles

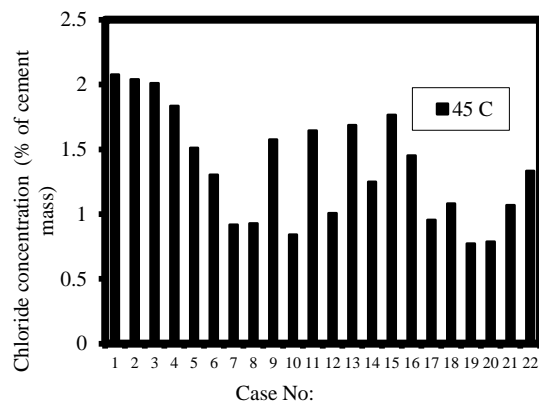


Figure 10. AS Cl⁻ concentration at 45 cycles

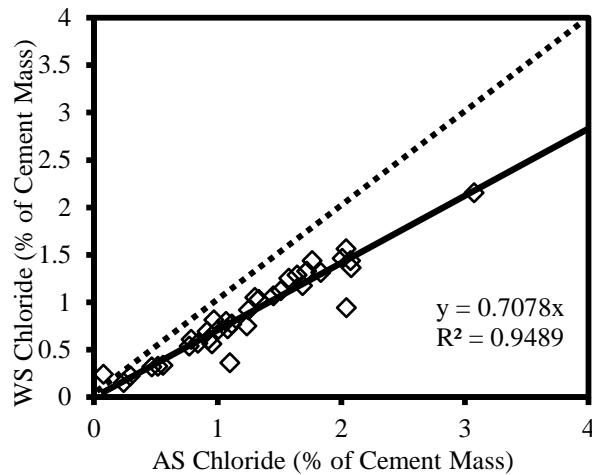


Figure 11. Water soluble Cl⁻ concentration VS acid soluble Cl⁻

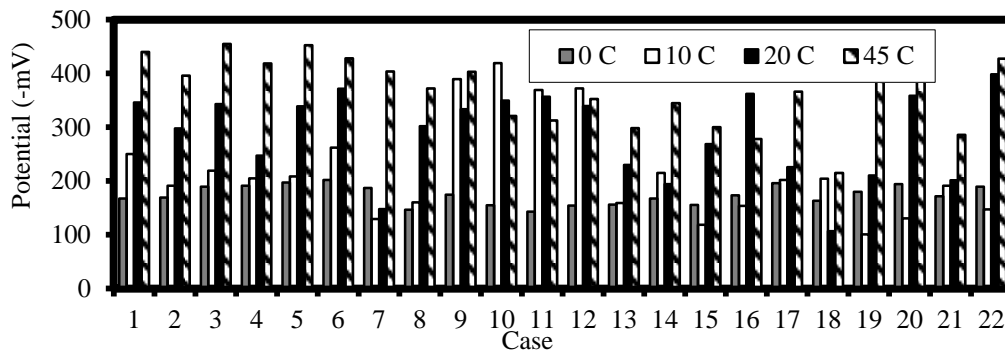
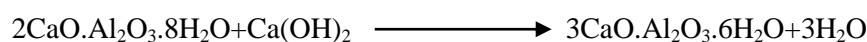
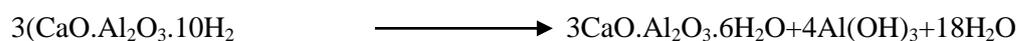


Figure 12. Half-cell potential at 0C, 10C, 20C, 45C

Micro-Cell Corrosion

The micro-cell corrosion current density of the steel bars is shown in Figure 13. Generally, the passivity limit is defined at a corrosion current density of $0.1 \mu\text{A}/\text{cm}^2$ (Andrade and Alonso, 2000). Before accelerated marine exposure, the corrosion current density was negligible. After 10 cycles of exposure, it was found that C1, C9, C10, C11, and C12 show corrosion current density over $0.1 \mu\text{A}/\text{cm}^2$. No coating was applied for C1. For C9, C10, C11, and C12, alumina cement paste coat was applied over the steel bar. After 20 cycles of exposure C9, C10, C11, and C12 show high amount of corrosion current density, also C1, C5, C6, C16 and C22 showed relatively more corrosion current density. After 45 cycles of exposure, same as the previous cycles C9, C10, C11, and C12 showed remarkably high amount of corrosion current density. Also other cases showed corrosion current density above passivity limit except for C13, C15, C18, and C21 for which the steel bars were coated with a low W/C, except the cases with alumina cement. The reason for more corrosion over the steel bar coated with alumina cement is due to the following conversion of hydration products:



The conversion reactions liberate water molecules and create more voids around the steel bar. For this reason, C9, C10, C11, and C12 showed more corrosion. Both seawater and tap water were used for making cement paste with alumina cement (Table 6). Both cases showed significant amount of corrosion over the steel bars.

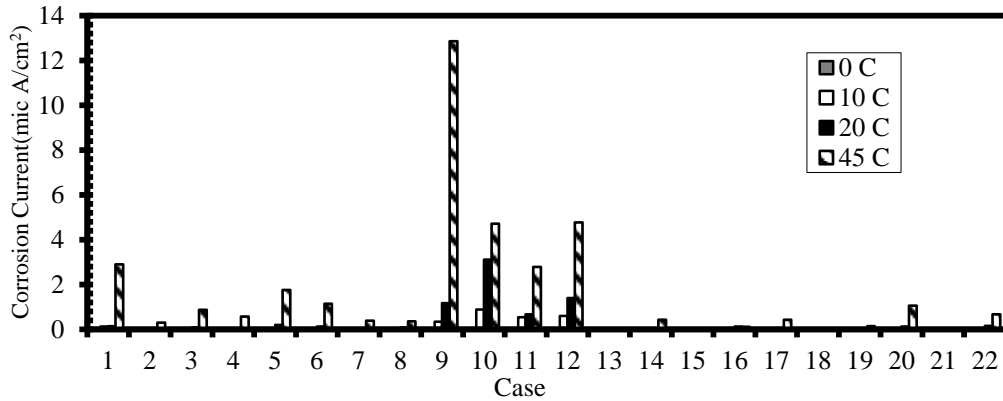


Figure13. Micro-cell corrosion at 0C, 10C, 20C, 45C

Concrete Resistance

Concrete resistances over the steel bar is shown in Figure 14. Before accelerated marine exposure (zero cycle), more concrete resistance over the steel bar is found for the cases for which cement-paste coating was applied over steel with a low W/C. No significant reduction of concrete resistance was found for C9, C10, C11, and C12. However, these cases showed more corrosion current density over the steel bars due to conversion reactions of hydration products as explained earlier.

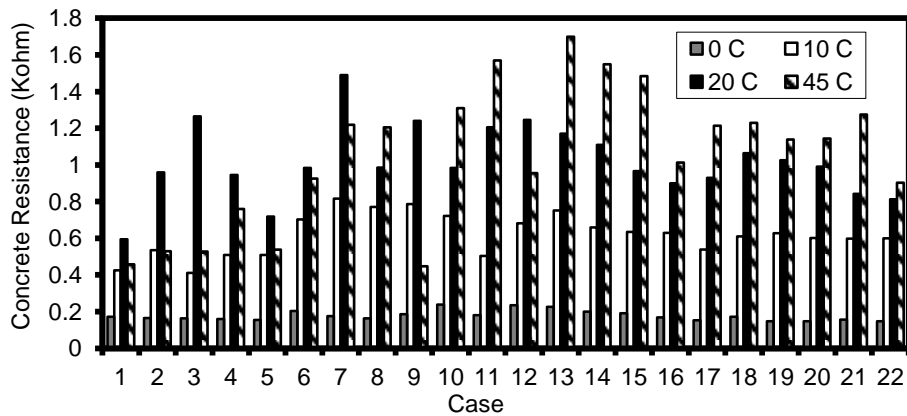


Figure14. Concrete resistance (Rc) at 0C, 10C, 20C, 45C

Anodic Polarization Curves

The anodic polarization curves of the steel bars were measured at 10, 20, and 45 cycles of exposure. The passivity grades of the steel were evaluated from the anodic polarization curves (Otsuki et al, 1992). The passivity grades are evaluated for qualitative comparisons of the anodic polarization curves. The more is the passivity grade, the better is the passivity around the steel bar. The results of passivity grade of steel bars are summarized in Table 8 after 10, 20, and 45 cycles of exposure. Alumina cement paste coated cases were found more

corrosive than the other cases. Higher passivity grades are found for the cases for which steel bar was coated with a low W/C.

Table 8. Passivity Grades of Steel Bars

Case	10 Cycle	20 Cycle	45 Cycle	Case	10 Cycle	20 Cycle	45 Cycle
C1	5	3	1	C12	5	2	5
C2	5	4	3	C13	5	5	5
C3	5	3	1	C14	5	5	3
C4	5	3	1	C15	5	4	3
C5	5	2	1	C16	5	3	3
C6	5	3	1	C17	5	4	3
C7	5	5	1	C18	5	5	5
C8	5	3	2	C19	5	4	3
C9	5	2	1	C20	5	3	2
C10	5	1	1	C21	5	4	5
C11	5	3	1	C22	5	3	1

Physical Observation, Corroded Area, and Pit Depth

After electrochemical investigations, the specimens were split opened to see the condition of the steel bars as well as the split opened concrete surface surrounding the steel bars. The results of physical evaluation of corrosion of the specimens at 10 cycles, 20 cycles, and 45 cycles are summarized in Table 9. The surface condition of the steel bars before and after removal of cement paste coating at 45 cycles is shown in Figure 15 and Figure 16. After 10 cycles, corrosion was found for C9, C10, C11, and C12. Rust spots were found for C6, C7, C8, C15, and C16. Whitish surface were found for other cases. After 20 cycles of exposure, it was found that C9, C10, C11, and C12 were corroded by 70%, 90%, 30%, and 60% of total surface area of steel bars, respectively. Some spots were found in C2 (2 spots), C4 (4 spots), C7 (1 spot), C8 (9 spot), C15 (1 spot), C16 (1 spot). For C5, corroded area over the steel bar was 0.5 cm². But no corrosion was found for C1, C3, C6, C13, C14, and C17~22. After 45 cycles of exposure it was found that steel bar of C9, C10, C11, C12 were fully corroded where alumina cement were used to make paste. C4, C5, C6, C8, C14, C15, C18, C19, C20, C21, and C22 were corroded by 14.4%, 13.6%, 18.1%, 3.8%, 11.1%, 10.5%, 0.6%, 0.3%, 45.1%, 0.9%, and 1.7% of total surface area of steel bar, respectively. No corrosion was found for the cases for which steel bars were coated with a low W/C.



Figure 15. Visual observation after split the specimen and before removing the paste (45 cycle)



Figure 16. Visual observation of steel bars after removing the cement paste

Table 9. Condition of Steel Surface After Split the Specimen

Case	10 Cycle	20 Cycle	45 Cycle
C1	Whitish surface	Slightly corroded	14.4% corroded
C2	Shiny surface, same as original surface	Two spots (1 mm and 0.5 mm dia)	No corrosion
C3	Whitish surface	No corrosion, same as initial, very shiny surface	No corrosion
C4	Uniform whitish surface on steel bar	4 spots (2 mm dia, 1 mm dia, 1.5 mm dia, and 0.5 mm dia)	Slightly corroded
C5	Whitish surface, spots	Corrosion over an area of 0.5 cm ²	13.6 % corroded
C6	Some spot, 5 spots in 50 mm length	No corrosion	18.1% corroded
C7	Some spot, 2 spot in 50 mm length	One spot (2 mm dia)	No corrosion
C8	Some spot, 4spot in 50 mm length	9 spots (less than 1 mm dia)	3.8 % corroded
C9	Corrosion, brownish hydration adhered on the surface	Corrosion over 70% area, brownish surface, rust in concrete, black colored corrosion at densely corroded regions	100 % corroded
C10	Corrosion, brownish hydration adhered on the surface	90% corrosion, and same as above	100 % corroded
C11	Some spots	30% corrosion	100 % corroded
C12	Corrosion, brownish hydration adhered on the surface	60% corrosion	100 % corroded
C13	Shiny surface, same as original surface	Very clean surface as initial	No corrosion
C14	One spot in 50 mm length	No corrosion	11.1 % corroded
C15	4 spots in 50 mm length	One spot (1 mm dia)	10.5 % corroded
C16	2 spots in 50 mm length	One spot 2 mm by 2 mm	No corrosion
C17	Whitish surface	No corrosion	No corrosion
C18	Whitish surface	No corrosion	0.6 % corroded
C19	Whitish surface	No corrosion	0.3 % corroded
C20	Whitish surface	No corrosion	45.1 % corroded
C21	Whitish surface	No corrosion	0.9 % corroded
C22	Whitish surface	No corrosion	1.7 % corroded

After 45 cycles of exposure, corrosion depth was measured after cleaning the steel bar. Corrosion depths are summarized in Table 10. Deepest corrosion pit was found for C15 and it was 0.35 mm. For C4, C8, C9, and C14, corrosion depths were found to be, 0.24 mm, 0.27

mm, 0.22 mm, and 0.29 mm respectively. Also very small corrosion depth was found for C1, C3, C5, C6, C10, C11, C16 and C17. No corrosion depth was found for C2, C7, C13, C18, C19, and C21.

After physical observation it was found that cement paste coating was effective to prevent corrosion of steel bars even for a high chloride level because the paste create a dense steel-concrete interface around the steel bars. Among the cement pastes, alumina cement paste is found to be ineffective because of conversion reactions. Ordinary portland cement paste was found very effective to prevent corrosion with a low W/C ratio. Also blended cement like, slag, flyash, silica fume, and metakaoline give good results to prevent corrosion of steel bars.

Table 10. Pit Depth on the Steel Surface

Case	Pit Depth (mm)	Case	Pit Depth (mm)
C1	0.24	C12	0.2
C2	No Pit	C13	No Pit
C3	Very small pit	C14	0.29
C4	Very small pit	C15	0.35
C5	Very small pit	C16	Very small pit
C6	Very small pit	C17	Very small pit
C7	No Pit	C18	No Pit
C8	0.27	C19	No Pit
C9	0.22	C20	0.12
C10	Very small pit	C21	No Pit
C11	Very small pit	C22	0.14

Optical Microscopic Investigation

To clarify the nature of the steel-concrete interface, optical microscope investigation on the steel-concrete interface was extensively carried out on the split-opened surface surrounding the steel bars. The split opened surface surrounding the steel bars for different cases are shown in **Figure 17**. Presence of voids was found for the uncoated steel bars, steel bars coated with a high W/C, and steel bars coated with alumina cement. These voids cause corrosion over the steel bars. It is clearly understood that the physical nature of the steel-concrete interface in concrete is very important to initiate corrosion over the steel bars.

Optical microscope investigation was carried out for largest void, small voids, rusted interface, and cracked interface. Large void was found in all cases and also a lot of small voids were found at the steel-concrete interface for all cases.

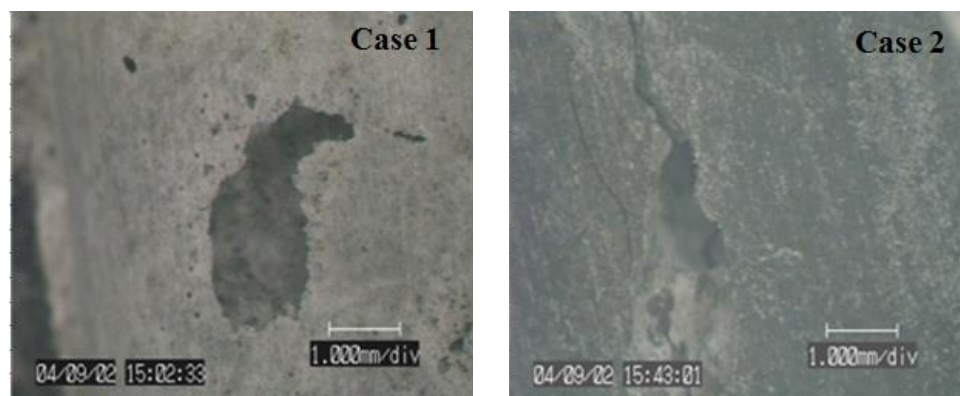


Figure 17(a). Steel-concrete interface under optical microscope (1-2)

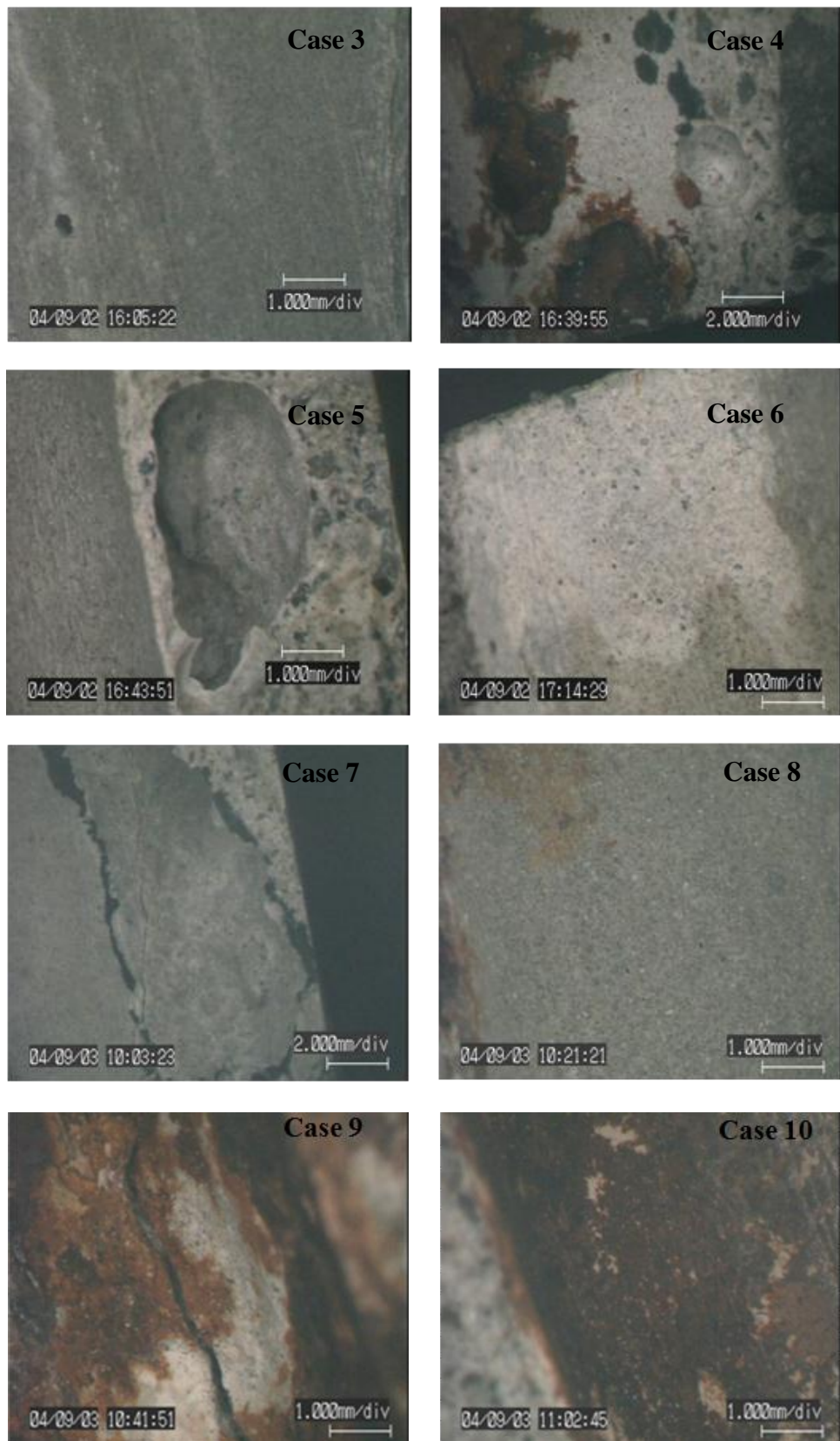


Figure 17(b). Steel-concrete interface under optical microscope (3-10)

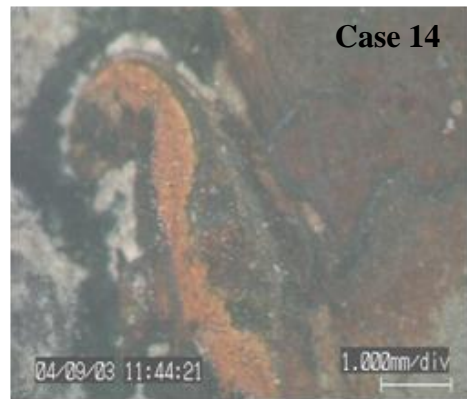


Figure 17(c). Steel-concrete interface under optical microscope (11-18)

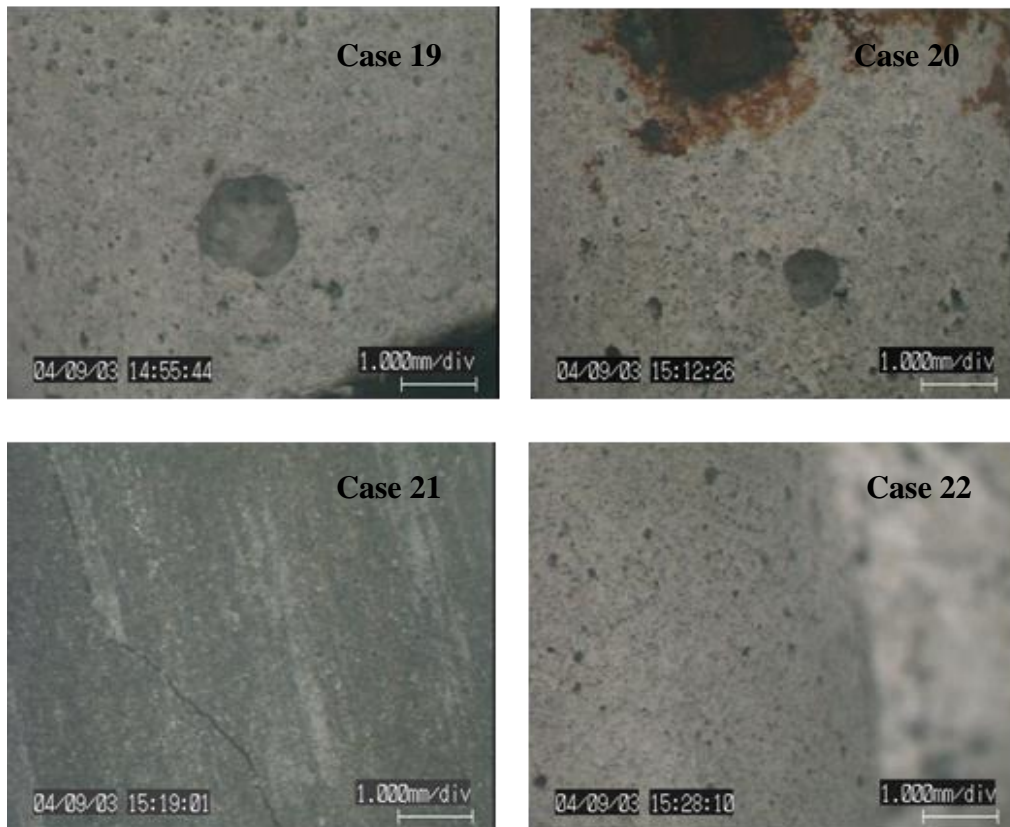


Figure 17(d). Steel-concrete interface under optical microscope (19-22)

CONCLUSIONS

The following conclusions are made based on the scope of experimental investigation conducted in this study:

1. Physical nature of steel-concrete interface plays a vital role in initiation of corrosion over the steel bar in concrete,
2. Application of a dense cement paste coat over the steel bar (with low W/C) enhances chloride threshold level significantly,
3. Alumina cement paste coat over the steel bar produces a porous interface due to conversion reactions,
4. The following relationship between water soluble (WS) chloride concentration and acid-soluble (AS) chloride concentration is proposed :

$$\text{Water soluble chloride concentration} = .708 \times \text{Acid Soluble Chloride Concentration}$$

5. For making sustainable marine reinforced concrete construction, cement paste coated steel bars may be used.

ACKNOWLEDGEMENTS

The authors wish to express their gratitude and sincere appreciation to the authority of Port and Airport Research Institute (PARI), Independent Administrative Institution, Yokosuka, Japan for giving support to perform this study.

REFERENCES

- Andrade, C., Alonso, C. (2000). "On-site Measurement of Corrosion Rate of Reinforcements." *Fifth CANMET/ACI International Conference on Durability of Concrete*, Barcelona, Spain, 171-183.
- Al-Tayyib, A. J.; Shamim Khan, M.; Allam, I. M.; and Al-Mana, A. I. (1990). "Influence of Pre-Rusting on Steel Corrosion in Concrete." *Cement and Concrete Research*, 20(6), 955-960.
- ASTM C876(1991). "Standard Test Methods for Half-Cell Potential of Uncoated Reinforcing Steel in Concrete." *American Society for Testing and Materials*, ASTM.
- Avial-Mendoza, J.; Flores, J. M.; and Castillo, U. C. (1994). "Effect of Superficial Oxides on Corrosion of Steel Reinforcement Embedded in Concrete." *Corrosion*, NACE International, 50(11), 879-885.
- Bradbury, P. C., and Double, D. D. (1976). "The Conversion of High Alumina Cement/Concrete." *Master. Sci. Eng.*, 23(1), 43-53.
- Brown, R.D. (1980). "Mechanism of Corrosion of Steel in Concrete in Relation to Design, Inspection and Repair of Offshore and Coastal Structures." *ACI SP*, 65, 169-204.
- Fontana, M. G., and Greene, N. D. (1983). *Corrosion Engineering*, McGraw-Hill, New York.
- Goni, S., Andrade, C., and Page, C. L. (1991). "Corrosion Behavior of Steel in High Alumina Cement Mortar Samples: Effect of Chloride." *Cement and Concrete Research*, 21(6), 635-646.
- Li, L., and Sagues, A. A. (2001). "Chloride Corrosion Threshold of Reinforcing Steel in Alkaline Solutions—Open-Circuit Immersion Tests." *Corrosion*, NACE International, 57(1), 19-28.
- Mohammed, T. U.; Fukute, T.; Yamaji, T.; and Hamada, H. (2002). "Long- Term Durability of Concrete Made with Different Water Reducing Chemical Admixtures Under Marine Environment." *Concrete for Extreme Condition*, Thomas Telford Publishing, UK, 233-243.
- Mohammed, T. U.; Otsuki, N.; and Hisada, M. (1999). "Corrosion of Steel Bars with Respect to Orientation in Concrete." *ACI Materials Journal*, 96(2), 154-159.
- Mohammed, T. U.; Otsuki, N.; Hamada, H.; and Yamaji, T. (2002). "Chloride-Induced Corrosion of Steel Bars in Concrete with Presence of Gap at Steel-Concrete Interface." *ACI Materials Journal*, 96(2), 149-156.
- Novak, P.; Mala, R.; and Joska, L. (2001). "Influence of Pre-Rusting on Steel Corrosion in Concrete." *Cement and Concrete Research*, 31, 589-593.
- Otsuki, N.; Nagataki, S.; and Nakashita, K. (1992). "Evaluation of AgNO₃ Solution Spray Method for Measurement of Chloride Penetration into Hardened Cementitious Materials." *ACI Materials Journal*, 89(6), 587-592.
- RILEM Committee 60-CSC (1987). "Corrosion of steel in concrete.", State of the Art Report, RILEM, Chapman and Hall, London.